

AE MONITORING OF CORROSION PROCESS IN REINFORCED CONCRETE UNDER CYCLIC WET AND DRY CONDITION

Yuma Kawasaki, Misuzu Kitaura, Yuichi Tomoda & Masayasu Ohtsu

Kumamoto University

Graduate School of Science and Technology

Kurokami 2-39-1

Kumamoto 860-8555

Japan

101d9107@st.kumamoto-u.ac.jp

KEYWORDS: Acoustic Emission, Corrosion, SiGMA Analysis, Salt Attack

ABSTRACT

Various deterioration and damage in reinforced concrete (RC) have been reported. Since salt is one of deterioration causes of RC, monitoring and diagnosis against deterioration are key issues. Thus, development of non-destructive evaluation (NDE) technique is important to assess corrosion process. To identify the onset of corrosion and the nucleation of corrosion-induced cracking in concrete due to expansion of corrosion products, continuous acoustic emission (AE) monitoring is available. In order to clarify these phenomena, cyclic wet and dry tests are performed in a laboratory. The SiGMA (Simplified Green's functions for Moment tensor Analysis) procedure is applied to AE waveforms to identify source kinematics of micro-crack locations, types and orientations. This study shows that the onset of corrosion and the nucleation of corrosion-induced cracking in concrete are visually identified. Then, cracking mechanisms due to the expansion of corrosion products are quantitatively clarified.

INTRODUCTION

In concrete engineering, it is a serious problem that concrete structures are no longer maintenance-free. In this respect, non-destructive evaluation (NDE) corrosion damage was reported (Dubravka et al., 2000). In reinforced concrete (RC) structures, passive films on the surface of rebars (reinforcing steel-bars) could be broken due to penetration of chloride ions, and activated ferrite ions lead to corrosion of rebars. Because almost all of concrete structures are reinforced by rebars, the corrosion due to salt attack has been referred to as the most critical deterioration of reinforced structures. So far, electrochemical techniques of the half-cell potentials and the polarization resistance are widely employed to evaluate corrosion of rebar. Recently, acoustic emission (AE) method has been introduced to detect corrosion-induced cracking in concrete (Ohtsu, 2003).

According to a phenomenological model of rebar corrosion in seawater environments, it is reported (Melchers et al., 2006) that a typical corrosion loss during the corrosion process can be divided into four phases shown in Fig. 1. At Phase 1, the onset of corrosion is initiated. The activity of the corrosion process is dominated by the rate of penetration of oxygen and water. Then a corrosion loss decreases at

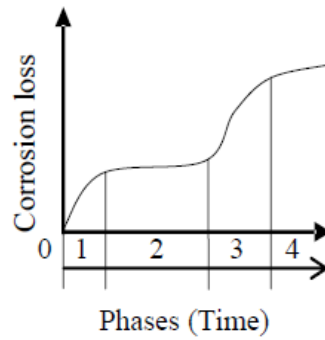


Fig. 1 Typical corrosion loss for steel in seawater immersion.

Phase 2, because the flow of oxygen is eventually inhibited by corrosion products of rebar. The corrosion process increases again at Phase 3, because the corrosion penetrates inside the rebar and the expansion of corrosion products occurs. Eventually, the corrosion of rebar progresses at an almost constant speed at Phase 4. Thus, the phenomenological model is referred to as a two-step process of the onset of corrosion and the expansion of corrosion products.

By applying AE techniques, it has been reported that the onset of corrosion and the nucleation of concrete cracking are detected (Ohtsu, 2003, Ohtsu and Tomoda, 2008). Consequently, continuous AE measurement is applied to identify the transition periods at the onset of corrosion and at the nucleation of concrete cracking. AE activities under cyclic wet and dry test are investigated and these results are confirmed by scanning electron microscope (SEM). To clarify micro-cracks in concrete, SiGMA (Simplified Green's functions for Moment tensor Analysis) procedure has been applied (Ohtsu, 1991, Ohtsu and Ohno et al., 2008). Kinematics of AE sources, such as crack location, crack type and crack orientation, in the corrosion process is analyzed by SiGMA analysis from recorded AE waveforms.

AE PARAMETER

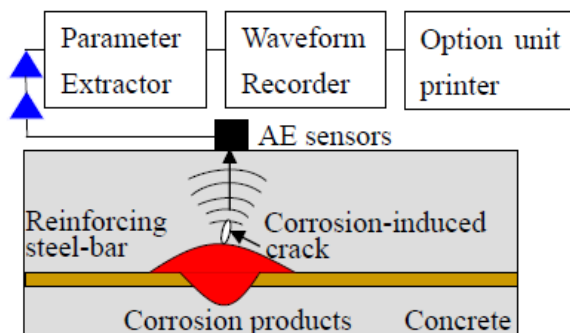


Fig. 2 AE generation due to corrosion of rebar.

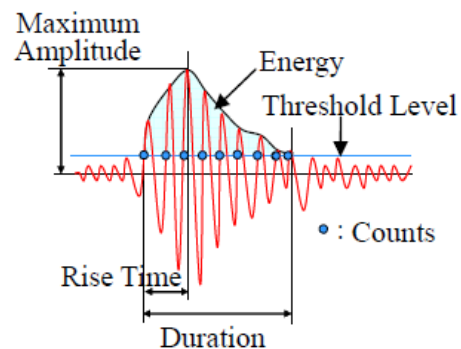


Fig. 3 AE waveform parameters.

AE detection due to the corrosion of rebar is illustrated in Fig. 2 (Ohtsu, 1996). AE events are associated with cracking and are detected by AE sensors as electrical signals, which are amplified, filtered, and processed. An AE signal is characterized by employing AE parameters such as energy, counts, event, amplitude, rise time and duration as illustrated in Fig. 3.

THORY OF SIGMA ANALYSIS

According to the generalized theory of AE (Ohtsu and Ono, 1984), AE signals are generated by micro-crack motions in a solid. The SiGMA analysis consists of 3-D (three-dimensional) AE source location procedure and moment tensor analysis for AE sources. In the SiGMA analysis, two parameters of the arrival time (P1) and the amplitude of the first motion (P2) shown in Fig. 4 are read and applied to the analysis.

In the location procedure, AE source (crack) location x' is determined from the arrival time differences t_i between the observation point x_i and x_{i+1} , by solving equations,

$$R_i - R_{i+1} = |x_i - x'| - |x_{i+1} - x'| = v_p t_i \quad (1)$$

Here, v_p is the velocity of P-wave. R is the distance between the source x' and the observation point x .

After determining the AE source location, the amplitudes of the first motion (P2) are substituted into the following equation.

$$A(x) = C_S \cdot \frac{\text{Ref}(t, \gamma)}{R} \cdot \gamma_p \gamma_q M_{pq} \cdot DA \quad (2)$$

Here, $A(x)$ is the amplitude of the first motion and C_S is the calibration coefficient of the sensor sensitivity and material constants. The reflection coefficient $\text{Ref}(t, \gamma)$ is obtained as t is the direction of sensor sensitivity. DA is area of crack surface, M_{pq} is the moment tensor and γ is the direction vector of distance R from the source to the observation point x as shown in Fig. 5.

The moment tensor M_{pq} consists of the crack motion vector l and the normal vector n to the crack surface. In an isotropic material, the moment tensor M_{pq} is derived from the following equation.

$$M_{pq} = (\lambda l_k n_k \delta_{pq} + \mu l_p n_q + \mu l_q n_p) \Delta V \quad (3)$$

Here, λ and μ are Lamé constants.

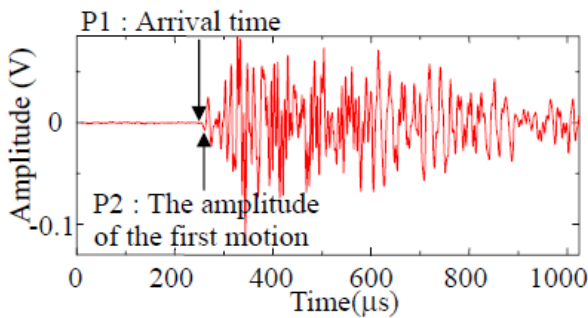


Fig. 4 Detected AE waveform.

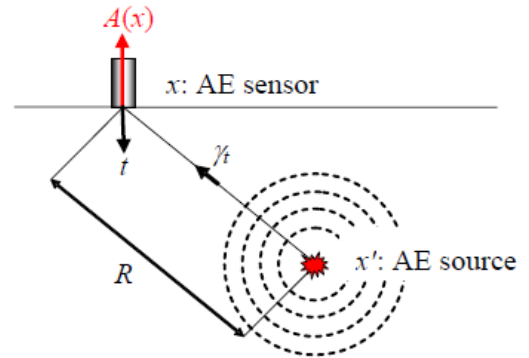


Fig. 5 Crack nucleation and AE detection.

To identify source kinematics, the eigenvalue analysis of the moment tensor has been proposed (Ohtsu, 1991). In general, the eigenvalues of the moment tensor are represented by the combination of the shear crack and the tensile crack as shown in Fig. 6. Eventually, the relative ratios X , Y and Z are obtained as,

$$1.0 = X + Y + Z$$

$$\frac{\text{the intermediate eigenvalue}}{\text{the maximum eigenvalue}} = 0 - Y/2 + Z \quad (4)$$

$$\frac{\text{the minimum eigenvalue}}{\text{the maximum eigenvalue}} = -X - Y/2 + Z$$

In the present SiGMA code, AE sources with shear ratios less than 40% are classified as tensile cracks. When the ratio X is larger than 60%, AE source is classified as a tensile crack. In the case of the ratios between 40% and 60%, the cracks are referred to as mixed-mode.

After determining the crack type, the direction of crack motion is derived from the eigenvectors. In the eigenvalue analysis, three eigenvectors e_1 , e_2 and e_3 ,

$$e_1 = l + n$$

$$e_2 = l \times n$$

$$e_3 = l - n$$
(5)

are also determined. Here, vector l and n are interchangeable. In order to visualize these kinematical information of AE sources, the Light Wave 3D software (New Tek) is introduced. Crack modes of tensile, mixed-mode and shear are given in Fig. 7. Here, an arrow vector indicates a crack motion vector l , and a circular plate corresponds to a crack surface which is perpendicular to a crack normal vector n .

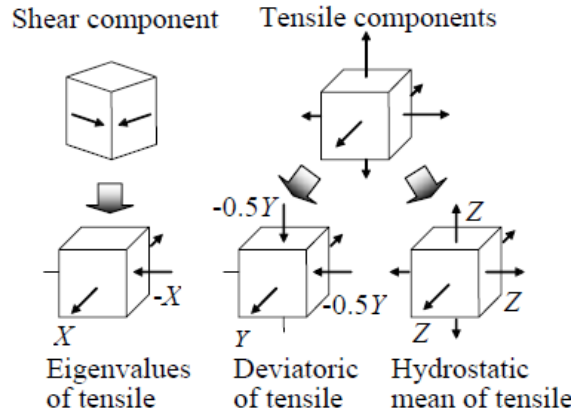


Fig. 6 Unified decomposition of eigenvalues of the moment tensor.

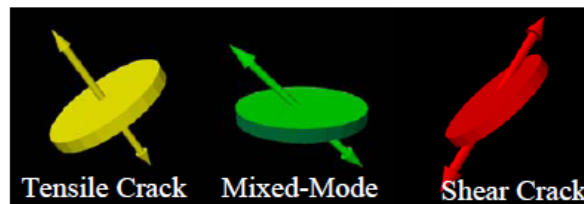


Fig. 7 3-D display models for tensile, mixed-mode and shear cracks.

EXPERIMENTS

RC specimens of dimensions 75×100×400 mm were made. Configuration of the specimen is illustrated in Fig. 8. A rebar of 13 mm diameter was embedded with 20 mm cover-thickness for longitudinal arrangement. Mixture proportion of concrete is given in Table 1. Here, NaCl solution is employed as mixed-water. Mechanical properties of hardened concrete are given in Table 2. Following the standard curing for 28 days, corrosion process under salt attack was simulated by cyclic wet and dry condition.

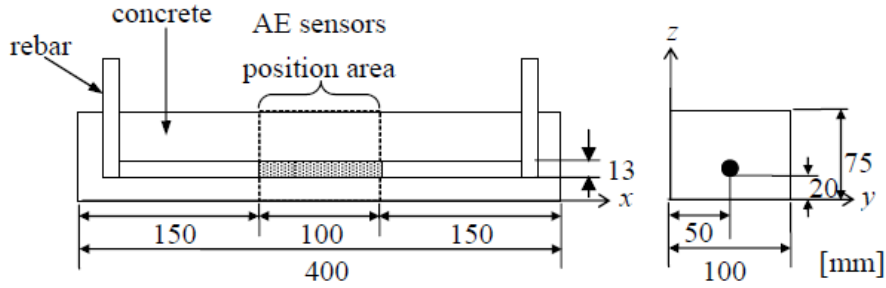


Fig. 8 Sketch of reinforced concrete specimen tested.

Table 1 Mixture proportion of concrete.

Maximum gravel size (mm)	Water to cement ratio W/C (%)	Weight per 1m ³ concrete					Slump (cm)	Air (%)
		Water (kg)	Cement (kg)	Sand (kg)	Gravel (kg)	NaCl (kg)		
10	55	185	336	823	1019	0.210	8	5

Table 2 Mechanical properties of hardened concrete.

Compressive strength (MPa)	Poisson's ratio	P-wave velocity (m/s)
43.9	0.2	4332

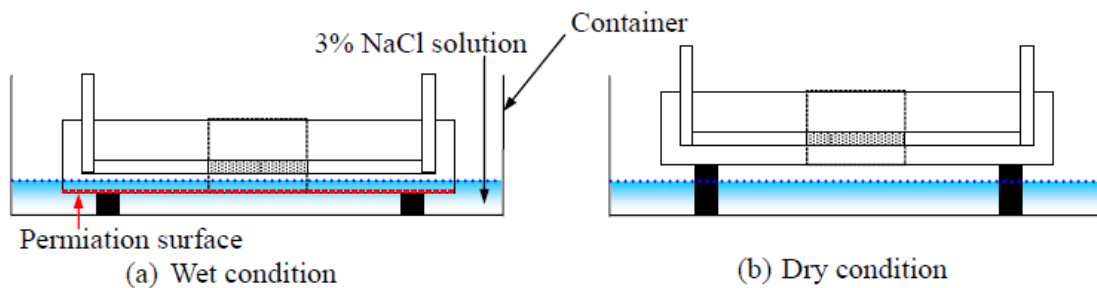


Fig. 9 Sketch of cyclic wet and dry test.

In the cyclic wet and dry test, the specimens were cyclically put into the container filled with 3% NaCl solution for a week and subsequently taken out of the container to dry under ambient temperature for another week as shown in Fig. 9. AE measurement was continuously conducted, by using AE measurement system (DiSP, PAC). Six AE sensors (R15, PAC) of 150 kHz resonance were attached to the

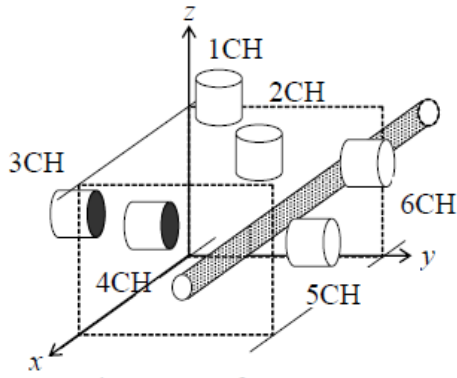


Fig. 10 Set of AE sensors.

Table 3 Coordinates of AE sensors.

	x (m)	y (m)	z (m)
1CH	0.010	0.030	0.075
2CH	0.100	0.070	0.075
3CH	0.090	0.000	0.045
4CH	0.020	0.000	0.030
5CH	0.095	0.100	0.033
6CH	0.010	0.100	0.055

surface of the specimen as shown in Fig. 10 and the coordinates of AE sensors are given in Table 3. The frequency range of the measurement was 10 kHz to 2 MHz and total amplification was 60 dB gain. For event counting, the dead-time was set to 2 msec and the threshold level was set to 40 dB gain. Every week, AE measurement was temporarily stopped for the electrochemical measurement.

Half-cell potentials at the surface of the specimen were measured by a portable corrosion meter, SRI-CM-II (Yokota al., 1999). Potentials were measured at one location on the bottom surface of the specimen. The specimen was measured every week. Then results of the half-cell potentials were converted to the probability of corrosion on the basis of ASTM C876 standard (ASTM, 1991), which is prescribed in Table 4.

Table 4 Criterion for half-cell potential (mV, CSE).

Potential	Corrosion probability
$-350\text{mV} < E$	90% no corrosion
$-350\text{mV} < E \leq -200\text{mV}$	Uncertain
$E < -350\text{mV}$	90% corrosion

RESULTS AND DISCUSSION

(1) AE Activity

Cumulative AE hits and AE events for every 1 hour of all 6 channels are shown in Fig. 11. An AE event corresponds to one phenomenon which was detected by all 6 AE sensors. AE hits and AE events start to gradually increase during the first 28th day. Then, AE hits have sharply-increased on the 28th day. From 42th day elapsed to 140th day, AE hits and AE events increase continually. The curve of cumulative AE hits is in remarkable agreement with the curve of corrosion loss in Fig. 1. Thus, it leads to the fact that the onset of corrosion started during the first 42nd day and the expansion of corrosion products occurred from 42nd day to 63rd day. It implies that AE events observed from 63rd day to 140th day could result from corrosion-induced cracking in concrete.

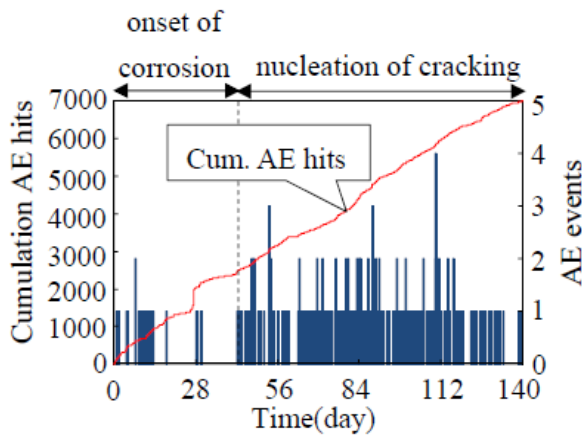


Fig. 11 Cumulation AE hits and AE events.

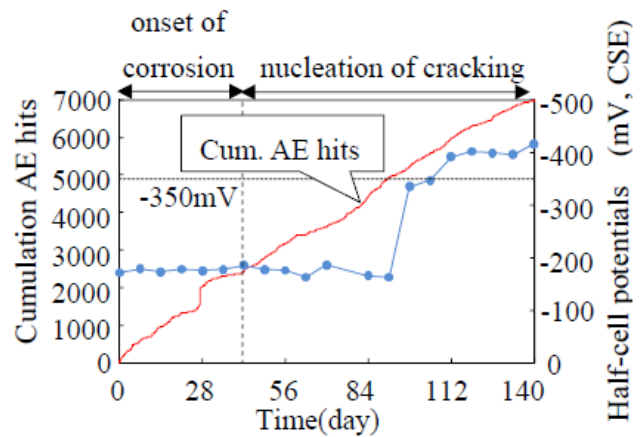


Fig. 12 Cumulation AE hits and Half-cell potentials.

(2) AE Activity and Half-cell Potentials

Cumulative AE hits are compared with half-cell potentials in Fig. 12. The half-cell potentials start to decrease after 91st day. After elapsed 112th day, the potentials became more negative than -350 mV. Thus, behaviors AE activity during the corrosion process is the earlier warning than the decrease trend of the half-cell potentials. The corrosion further penetrates inside. After 91st day elapsed, rust breaking and other internal cracks inside rebar could occur. Then, concrete cracks are nucleated due to expansion of corrosion products in rebar.

(3) SEM Observation

For SEM (JEOL JSM-5600), observation of rebars was conducted by taking rebar out of the specimen after 35th day elapsed and 105th day elapsed. Rust could be found at 35th day elapsed and 105th day elapsed by visual observation. SEM photo after 35th day is shown in Fig. 13 and SEM photo after 105th day is shown in Fig. 14. At the 35th day elapsed in Fig. 13, no corrosion is identified inside the rebar. At the 105th day elapsed in Fig. 14, the surface oxide film almost exfoliated and the rust on the superficial of the rebar under an oxide film is identified. Here, the magnifying power of a photo of Fig. 13 is 500. In Fig. 14, the magnifying power of a photo is 1000.

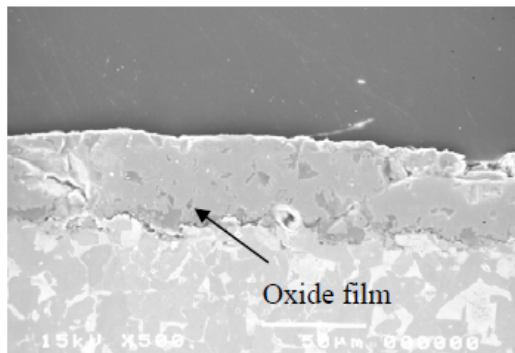


Fig. 13 At 35th day Cross-section SEM.

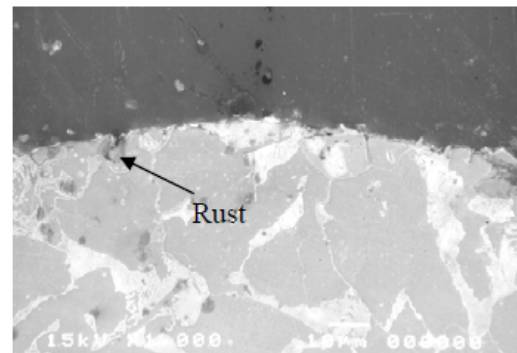


Fig. 14 At 105th day Cross-section SEM.

(4) SiGMA Analysis

In the SiGMA analysis, AE event definition time (EDT) is set to 100 μ sec. EDT is applied to recognize AE waves occurring within the specified time from the first-hit and to classify them as part of the current event. Results of the SiGMA analysis during the first 42nd day are illustrated in Fig. 15. At the period, only 10 AE events are determined. These events are located mostly surrounding the rebar. Results of the SiGMA analysis from 42nd day to 140th day are illustrated in Fig. 16. At the period, 159 AE events are determined. Large numbers of AE events are observed around the rebar. At 126th day, surface cracks were visually found. AE cluster at the total is compared with the surface crack observed at the bottom of the specimen in Fig. 17. Locations and orientations of AE sources are in remarkable agreement with the surface cracks observed. This suggests that generation of the corrosion-induced cracking in concrete could be visualized by conducting the SiGMA analysis continuously.

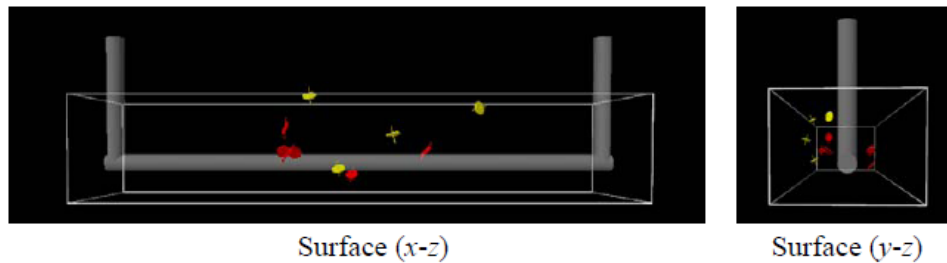


Fig. 15 Results of SiGMA analysis (0-42nd days)

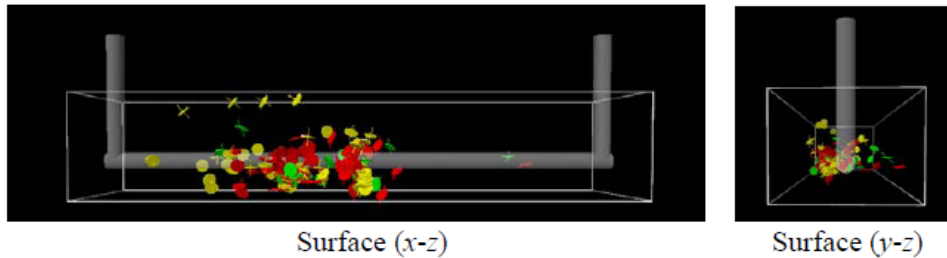


Fig. 16 Results of SiGMA analysis (42nd-140th days)

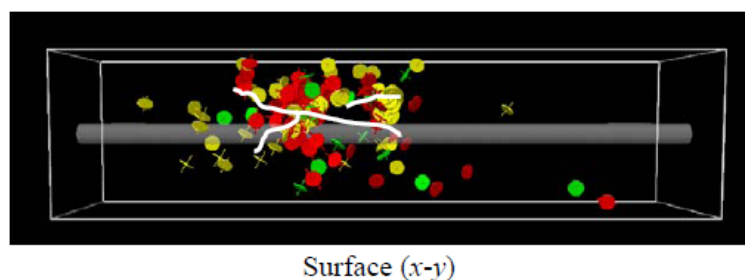


Fig. 17 Results of SiGMA analysis with cracks (Total days)

(5) Location Analysis

In the Location analysis, the AE event is applied which was detected by out of 5 AE sensors from all 6 AE sensors. AE event definition time (EDT) is set to 100 μ sec. Results of the Location analysis during the first 42nd day are illustrated in Fig. 18. During the first 42nd day elapsed, 40 AE events are observed at around the rebar. In the onset of corrosion, it implies that corrosion of rebar was able to be identified by



Fig. 18 Results of Location analysis (0-42nd days)

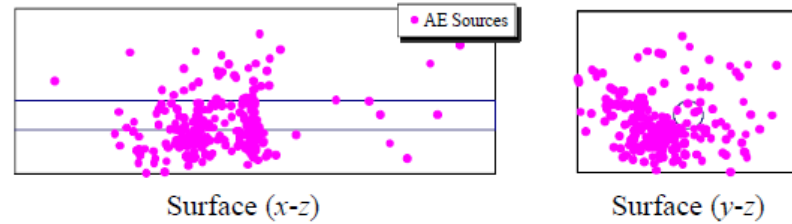


Fig. 19 Results of Location analysis (42nd-140th days)

Location analysis. Results of the Location analysis from 42nd day to 140th day are illustrated in Fig. 19. From 42nd day to 140th day elapsed, 247 AE events are observed from the rebar toward the surface of the specimen. It implies that those cracks progressed at the left of the specimen.

CONCLUSION

In order to clarify the deterioration process due to corrosion of reinforced concrete, AE monitoring is applied to the cyclic wet and dry test. The following conclusions are obtained.

1. In the cyclic wet and dry test, on deterioration process of a RC, the onset of corrosion and the nucleation of corrosion-induced cracking in concrete are distinguished from AE activity. This confirms that these two stages can be identified by AE monitoring.
2. From SEM, comparing SEM photos with AE activity, it is summarized that at 35 days AE activity corresponds to the transition from Phase 1 to Phase 2, and at 105 days AE activity is associated with the transition from Phase 3 to Phase 4.
3. AE activity is low at the onset of corrosion. Thus, the number of AE events located a few. Then, AE sources clearly observed at the nucleation of cracking that the cracks occurred around the rebar. Results of SiGMA analysis during the corrosion process are in remarkable agreement with locations of the surface cracks. Results show that corrosion-induced cracking can be identified by the SiGMA analysis of AE monitoring.
4. In the Location analysis, AE events located around rebar at the onset of corrosion. Thus, it implies that early-warning of corrosion-induced cracking can be identified by the Location analysis of AE monitoring.

REFARENSES

- Dubravka., B. Dunja, M. and Dalibor, S. 2000. "Non-Destructive Corrosion Rate Monitoring for Reinforced Concrete Structures," *15th WCNDT*.
- Ohtsu, M. 2003. "Detection and Identification of Concrete Cracking in Reinforced Concrete by AE," Review of Progress in Quantitative NDE. *AIP conference 2003*, Proc.657, 22B, 1455-1462.
- Melchers, R. E. and Li, C. Q. 2006. "Phenomenological Modeling of Reinforcement Corrosion in Marine Environments," *ACI Materials Journal*, Vol. 103, No.1, 25-32.
- Ohtsu, M. and Tomoda, Y. 2008. "Phenomenological Model of Corrosion Process in Reinforced Concrete identified by AE," *ACI Materials Journal*, Vol. 105, No.2, 194-199.
- Ohtsu, M. 1991. "Simplified Moment Tensor Analysis and Unified Decomposition of Acoustic Emission Source : Application to In Situ Hydrofracturing Test," *J. of Geophysical Research*, Vol. 96, No. B4, 6211-6221.
- Ohno, K., Simozono, S., Sawada, Y. and Ohtsu, M. 2008. "Mechanisms of Diagonal-Shear Failure in Reinforced Concrete Beams analyzed by AE-SiGMA," *J. of Solid Mechanics and Materials Engineering*, Vol. 2, No. 4, 462-472.
- Ohtsu, M. 1996. "The History and Development of Acoustic Emission in Concrete Engineering," *Magazine of Concrete Research*, 48(177), 321-330.
- Ohtsu, M. and Ono, K. 1984. "A generalized Theory of Acoustic Emission and Green's functions in a Half Space," *J. of Acoustic Emission*, Vol. 3, No.1, 124-133.
- Yokota, M. 1999. "Study on Corrosion Monitoring of Reinforcing Steel Bars in 36 Years-old Actual Concrete Structures," *Concrete library of JSCE*, 33, 155-164.
- ASTM C876. 1991. "Standards Test Method for Half-cell Potentials of uncoated Reinforcing Steel in Concrete," *Annual book of ASTM Standard*.